

The dynamics of the spreading of liquids on a solid surface. Part 2. Surfactants

By R. G. COX

Department of Civil Engineering and Applied Mechanics,
McGill University, Montreal, PQ, Canada

(Received 25 August 1983 and in revised form 2 December 1985)

A theoretical study is made of the effect of the presence of a surfactant on the dynamics involved in the movement of the contact line when one liquid displaces an immiscible second liquid where both are in contact with a smooth solid surface. The general procedure of solution is described for a general model for slip between solid and liquid near the contact line and also for a general macroscopic geometry. For small capillary number and for small values of the length over which slip occurs, it is shown, using singular perturbation analysis, that either 2 or 3 regions of expansion are necessary depending on the type of limiting process being considered. Solutions are obtained for both situations but for the more important three-region expansion case (where there can be large dynamic effects), a detailed discussion is given of the manner in which the observable macroscopic contact angle is shown to depend on the contact line velocity and on surfactant concentration. The conditions of validity for the theory are also discussed.

1. Introduction

Consider two immiscible liquids (A and B) or a liquid and a gas in contact with a solid surface and suppose that liquid A displaces liquid B so that the contact line (where the liquid–liquid interface intersects the solid surface) is constrained to move across the solid surface with velocity U . It is experimentally observed that the contact angle (that the liquid–liquid interface makes with the solid surface) measured through liquid A increases as U is increased [Dussan V. 1979]. For the situation where there is no surfactant present (so that there is continuity of tangential stress across the interface), the dynamics of this problem has been examined by Cox (1986). The present paper follows this earlier work very closely and extends the results to situations where an insoluble surfactant is present on the liquid–liquid interface. As with the earlier work, it is assumed that the solid surface (or surfaces) involved are perfectly smooth and chemically homogeneous and that we consider a system of completely general geometry.

It is well known that [Hocking 1977; Huh & Mason 1977; Lowndes 1980], whether or not surfactant is present, it is necessary to postulate slip between the liquids and the solid surface (or possibly some other mechanism) at small distances, or order s say, from the contact line. This is because there is otherwise a non-integrable singularity in the stress at the contact line which would give rise to an infinite drag force on the solid surface.

For any specific model for this slip and a given overall geometry of the system, the flow fields, surfactant concentration and interface shape are obtained for small capillary number Ca and small ratio ϵ of slip length s to macroscopic lengthscale. After

a discussion of the outer region (§3) valid everywhere except close to the contact line in which the overall geometry of the system is important and the inner region (§4) applicable at distances of order s from the contact line, it is shown in §5 that in the same manner as for the surfactant-free situation (Cox 1986) there are either 2 or 3 regions of expansion necessary depending on the limiting process involved. For the latter situation of 3 regions, an intermediate region exists between the inner and outer regions. It is shown that for situations where the two-region expansion is applicable, the predicted contact angle must always be approximately its static value whereas for the three-region expansion large dynamic effects are predicted. Thus in §6 and §7 the solution for the three-region expansion problem is obtained from which it is found that at lowest order in capillary number, this solution is independent of the solution in the inner and outer regions and is therefore independent of the slip model chosen and of the overall geometry of the system being considered. Furthermore, even at the next higher order in the capillary number, the solution is dependent only upon two constants obtained from matching onto the inner region (and thus depend on the slip model used) and two constants obtained from matching onto the outer region (and thus depend on the overall geometry of the system). Finally in §8 a discussion of the results obtained is given together with details concerning the conditions of validity of the specific assumptions made regarding the surfactant behaviour.

2. General problem

Consider a situation in which liquid A (of viscosity μ_A and density ρ_A) displaces liquid B (of viscosity μ_B and density ρ_B). In a manner similar to that described by Cox (1986), it will be assumed that the slip length s is much smaller than a characteristic macroscopic lengthscale R so that

$$\epsilon \equiv \frac{s}{R} \ll 1, \quad (2.1)$$

and also that interfacial tension effects dominate over viscous effects so that

$$Ca \equiv \frac{\mu_A U}{\sigma^*} \ll 1, \quad (2.2)$$

where U is a characteristic velocity of the spreading process and σ^* a characteristic interfacial tension of the liquid-liquid interface. It is in terms of these two small parameters ϵ and Ca that expansions will be made using singular perturbation methods. Whereas Cox (1986) considered a surfactant-free interface between the two liquids so that the tangential stress in the liquids was continuous across the interface, we consider here a surfactant being present so that the liquids can now exert a net tangential stress on the interface, this being balanced by a gradient of the liquid-liquid interfacial tension resulting from a gradient in surfactant concentration on the interface. For simplicity we shall assume that conditions are such that (a) the interfacial stress is isotropic and given by an interfacial tension σ which is a function only of the surfactant concentration c and does not depend on the flow at the interface, (b) the surfactant can be considered insoluble in the sense that there is negligible flux of the surfactant from the bulk of the fluids to the interface and vice-versa during the spreading process, (c) the surfactant is not deposited on the solid surface from the moving liquid-liquid interface, (d) the diffusion of surfactant along the interface is negligible compared with convection and (e) the concentration c of the surfactant is non-zero but finite at all points on the liquid-liquid interface during

the spreading process. A discussion is given in §8 of the relationship between these assumptions and the fluid mechanics involved from which various conditions for their validity are obtained.

It will also be assumed that the Reynolds numbers $(\rho_A RU/\mu_A)$ and $(\rho_B RU/\mu_B)$ for the flow in the liquids A and B are so small that inertia effects may be neglected and also that the Bond number $B \equiv |\rho_A - \rho_B|gR^2/\sigma^*$ is small so that gravity effects are negligible.

3. Outer region

Let c^* be the surfactant concentration corresponding to the characteristic interfacial tension σ^* . Then if a dimensionless concentration c and interfacial tension σ are defined as

$$c = \frac{c'}{c^*}, \quad \sigma = \frac{\sigma'}{\sigma^*}, \quad (3.1)$$

where c' and σ' are the dimensional values, the assumption (a) mentioned in §2 implies that $\sigma = \sigma(c)$ where $\sigma = 1$ for $c = 1$.

An outer region of expansion is defined in the same manner as Cox (1986) using variables made dimensionless by the quantities R , U and μ_A , so that it is valid everywhere except close to the contact line. Thus if \mathbf{u}_A and p_A are the dimensionless velocity and pressure in liquid A and \mathbf{u}_B and p_B the dimensionless velocity and pressure in liquid B in this outer region, then

$$\nabla^2 \mathbf{u}_A - \nabla p_A = 0, \quad \nabla \cdot \mathbf{u}_A = 0, \quad (3.2)$$

$$\text{in liquid A and} \quad \lambda \nabla^2 \mathbf{u}_B - \nabla p_B = 0, \quad \nabla \cdot \mathbf{u}_B = 0, \quad (3.3)$$

in liquid B where $\lambda = \mu_B/\mu_A$ is the viscosity ratio. Also \mathbf{u}_A and \mathbf{u}_B must satisfy on all solid walls:

- (i) zero normal component;
- (ii) the given slip boundary condition.

In addition, on the interface between the two liquids, the following conditions must apply:

(iii) the kinematic boundary condition relating the velocity at the interface to the interface motion;

(iv) the continuity of tangential velocity;

(v) the force balance on the interface in the tangential direction, which in our outer variables, gives

$$Ca (\tau_{tA} + \tau_{tB}) = -\nabla_2 \sigma, \quad (3.4)$$

where τ_{tA} and τ_{tB} are the tangential stresses on the interface due to liquids A and B, Ca is the capillary number defined by (2.2) and ∇_2 is the two-dimensional gradient operator in the liquid-liquid interface;

(vi) the force balance on the interface in the normal direction, which in outer variables is

$$\Delta P + Ca (\tau_{nA} + \tau_{nB}) = -\sigma \kappa, \quad (3.5)$$

where τ_{nA} and τ_{nB} are the normal components of stress on the interface due respectively to the flow in liquids A and B (directed from liquid A to liquid B) and κ is the curvature of the liquid-liquid interface (defined as positive with centres of curvature on the liquid B side of the interface).

The quantity ΔP appearing in (3.5) is the static pressure drop across the interface

(in going from liquid A to liquid B) made dimensionless by σ and R (instead of by μ_A , R and U) in order to make it of order unity.

In addition the interfacial tension σ is related to the surfactant concentration c by

$$\sigma = \sigma(c), \quad (3.6)$$

with the equation of continuity for the surfactant in the interface as

$$\nabla_2 \cdot (c \mathbf{u}) + \frac{\partial c}{\partial t} = 0. \quad (3.7)$$

In deriving (3.7) use is made of the assumptions (b) and (d) mentioned in §2. We shall throughout this paper use subscripts A and B on symbols referring to liquids A and B. However where no subscript is given, the quantity may be taken to refer to either liquid.

In order to examine what boundary conditions, if any, should be imposed on the velocity at the liquid–liquid interface as the contact line is approached, we take some general point O on the contact line and consider the motion in the neighbourhood of O relative to the moving interface. Let s be a unit vector at O in the tangent direction to the contact line and t be a unit vector perpendicular to s in the tangent plane at O to the liquid–liquid interface. Then if the component $\mathbf{u} \cdot s$ of the velocity \mathbf{u} in the direction s on the interface is *not* equal to the component $\mathbf{u}_w \cdot s$ of velocity \mathbf{u}_w of the solid surface at O in the direction of s , a velocity field proportional to r^0 would be generated in the liquids near the contact line (where r is distance from the contact line). This would then give rise to shear stresses proportional to r^{-1} in the s -direction on the liquid–liquid interface. Such a stress field would not be irrotational and could not therefore satisfy (3.4). Thus the assumption that $\mathbf{u} \cdot s \neq \mathbf{u}_w \cdot s$ was incorrect so that

$$\mathbf{u} \cdot s = \mathbf{u}_w \cdot s, \quad (3.8)$$

at the contact line. Since the surfactant is convected with the liquid velocity at the interface and is not deposited on the solid surface (assumptions (c) and (d) mentioned in §2), it follows that

$$\mathbf{u} \cdot t = 0. \quad (3.9)$$

Thus combining (3.8) and (3.9) it is seen that relative to the moving interface

$$\mathbf{u} = \mathbf{u}_w \cdot s s, \quad (3.10)$$

or relative to a fixed set of axes the velocity of the liquids at the interface is

$$\mathbf{u} = \mathbf{u}_c - \mathbf{u}_c \cdot s s + \mathbf{u}_w \cdot s s, \quad (3.11)$$

where \mathbf{u}_c is the velocity of the contact line and \mathbf{u}_w is now the velocity of the solid surface relative to the new fixed set of axes.

In the above equations (3.2) and (3.3) and boundary conditions [(i)–(vi), (3.6), (3.7) and (3.11)] for \mathbf{u} , the quantity ϵ will only appear in the slip boundary condition (ii). Also from the manner in which Ca appears, the velocity \mathbf{u}_A (or \mathbf{u}_B) may be expanded in the form

$$\mathbf{u}_A = \mathbf{u}_{A0} + Ca \mathbf{u}_{A1} + \dots, \quad (3.12)$$

while the liquid–liquid interface expressed as $f(\mathbf{r}) = 0$ [where \mathbf{r} is the position vector in outer variables], may be expanded as

$$f \equiv f_0 + Ca f_1 + \dots = 0. \quad (3.13)$$

The curvature κ of this interface and the quantities σ and c may likewise be expanded as

$$\kappa = \kappa_0 + Ca \kappa_1 + \dots, \tag{3.14}$$

$$\sigma = \sigma_0 + Ca \sigma_1 + \dots, \tag{3.15}$$

$$c = c_0 + Ca c_1 + \dots. \tag{3.16}$$

In the above expansions, \mathbf{u}_{A0} , \mathbf{u}_{A1} , f_0 , etc, may depend on ϵ . If these expansions are substituted into the above stated equations and boundary conditions for \mathbf{u} and like powers of Ca equated, then at lowest order (3.4) gives $\nabla_2 \sigma_0 = 0$ so that

$$\sigma_0 = \sigma_m, \quad c_0 = c_m, \tag{3.17}$$

where σ_m and c_m are functions only of time t and are related to each other by (3.6). Likewise the normal-stress boundary condition (3.5) at lowest order gives

$$\Delta P = -\sigma_m \kappa_0, \tag{3.18}$$

so that $f_0 = 0$ is just a static configuration of the interface with constant interfacial tension σ_m . The equation (3.7) at lowest order, namely

$$c_m \nabla_2 \cdot \mathbf{u}_0 = -\frac{\partial c_m}{\partial t}, \tag{3.19}$$

may then be integrated over the entire liquid-liquid interface area to give

$$c_m A = \text{constant}, \tag{3.20}$$

where A is the area of the interface (which has been assumed to be bounded). Thus in problems where the interface area does not change (such as the movement of a meniscus with constant velocity along a tube), c_m and hence σ_m are constants whereas in problems where A does change (such as the spreading of a drop of constant volume on a planar solid surface), c_m varies in time being inversely proportional to A , with σ_m then being determined by the relation (3.6). The zeroth-order velocity fields \mathbf{u}_{A0} , \mathbf{u}_{B0} are then determined by equations of the form (3.2) and (3.3), by the following boundary conditions on all solid surfaces:

(a) zero normal components of velocity;

(b) the given slip boundary condition;

and by the following boundary conditions on the static interface shape $f_0 = 0$:

(c) the kinematic boundary condition;

(d) the continuity of tangential velocity;

$$(e) \quad \nabla_2 \times (\boldsymbol{\tau}_{tA0} + \boldsymbol{\tau}_{tB0}) = 0 \tag{3.21}$$

obtained from (3.4) where $\boldsymbol{\tau}_{tA0}$ and $\boldsymbol{\tau}_{tB0}$ are the coefficients of Ca^0 in the expansions for $\boldsymbol{\tau}_{tA}$ and $\boldsymbol{\tau}_{tB}$:

$$(f) \quad \nabla_2 \cdot \mathbf{u}_0 = -\frac{1}{c_m} \frac{\partial c_m}{\partial t} = +\frac{1}{A} \frac{dA}{dt}, \tag{3.22}$$

obtained from (3.19) and (3.20).

In addition, from (3.11), we require on the interface as the contact line is approached that

$$\mathbf{u}_0 \rightarrow \mathbf{u}_c - \mathbf{u}_c \cdot \mathbf{ss} + \mathbf{u}_w \cdot \mathbf{ss}. \tag{3.23}$$

If \mathbf{u}_0 is expanded in terms of ϵ , then at order ϵ^0 the above boundary condition (b) becomes one of zero tangential velocity (see Cox 1986).

Once the flow field \mathbf{u}_0 has been determined, the correction σ_1 to the interfacial tension is determined by (3.4) at order Ca^{+1} , namely

$$-\nabla_2 \sigma_1 = \tau_{tA0} + \tau_{tB0}. \quad (3.24)$$

Then c_1 is obtained from (3.6) at order Ca^{+1} as

$$c_1 = \left\{ \frac{d\sigma}{dc} \Big|_{c_m} \right\}^{-1} \sigma_1, \quad (3.25)$$

and the shape correction from (3.5) as

$$\sigma_m \kappa_1 = -(\tau_{nA0} + \tau_{nB0}) - \sigma_1 \kappa_0, \quad (3.26)$$

where κ_1 is the curvature correction.

Since it is very difficult to solve this problem even for the most simple geometry and since we are primarily interested here in what happens close to the contact line, we will calculate only the asymptotic form of the solution as the contact line is approached since it is this which is needed for the matching procedure close to the contact line. At a general position on the contact line, we set up a cylindrical polar coordinate system (r, ϕ, z) in outer variables with origin O on the Ca^0 position of the contact line (and moving with the contact line) and z -axis lying along the tangent direction to the Ca^0 position of the contact line with $\phi = 0$ in the solid surface in the direction of liquid A (and opposite to that of the contact line motion for $U > 0$). For the purpose of investigating the flow in the neighbourhood of O , we can choose the characteristic speed U as the speed of the contact line at O , so that the solid surface moves with unit dimensionless velocity in the direction $\phi = 0$.

As $r \rightarrow 0$, the static interface shape $f_0 = 0$ may be written (Cox 1986) as

$$\theta = \{\theta_m + O(r)\} + O(Ca), \quad (3.27)$$

where θ is the slope angle that the interface makes with the solid surface at a general position and where θ_m is an unknown angle which will be referred to as the macroscopic contact angle. Even if the configuration of the liquid-liquid interface is time-dependent with characteristic time T , this unsteadiness has negligible effect (Cox 1986) on the normal stresses on the interface for $r \rightarrow 0$ if

$$T \text{ is of order } \frac{R}{U} \text{ or larger.} \quad (3.28)$$

Thus the kinematic boundary condition on the interface (i.e. boundary condition (c)) may be replaced by one of zero normal velocity. Solving for the velocity field \mathbf{u}_0 in the same manner as Cox (1986) it is seen that it may be expressed in terms of stream functions ψ_A and ψ_B (in liquids A and B) so that the radial component $(u_{A0})_r$ and transverse component $(u_{A0})_\phi$ of \mathbf{u}_{A0} may be written as

$$(u_{A0})_r = \frac{1}{r} \frac{\partial \psi_A}{\partial \phi}, \quad (u_{A0})_\phi = -\frac{\partial \psi_A}{\partial r}, \quad (3.29)$$

with similar expressions for \mathbf{u}_{B0} . By substituting into (3.2), (3.3) and the boundary conditions and solving, we obtain the values of ψ_A and ψ_B as

$$\left. \begin{aligned} \psi_A &= r\{(C_A \phi + D_A) \cos \phi + (E_A \phi + F_A) \sin \phi\}, \\ \psi_B &= r\{(C_B \phi + D_B) \cos \phi + (E_B \phi + F_B) \sin \phi\}, \end{aligned} \right\} \quad (3.30)$$

where the constants $C_A, D_A, E_A \dots$ are

$$\left. \begin{aligned} C_A &= -\frac{\sin^2 \theta_m}{\theta_m^2 - \sin^2 \theta_m}, \\ D_A &= 0, \\ E_A &= \frac{\sin \theta_m \cos \theta_m - \theta_m}{\theta_m^2 - \sin^2 \theta_m}, \\ F_A &= \frac{\theta_m^2}{\theta_m^2 - \sin^2 \theta_m}, \\ C_B &= -\frac{\sin^2 \theta_m}{(\pi - \theta_m)^2 - \sin^2 \theta_m}, \\ D_B &= \frac{\pi \sin^2 \theta_m}{(\pi - \theta_m)^2 - \sin^2 \theta_m}, \\ E_B &= \frac{\sin \theta_m \cos \theta_m + (\pi - \theta_m)}{(\pi - \theta_m)^2 - \sin^2 \theta_m}, \\ F_B &= \frac{-\pi \sin \theta_m \cos \theta_m - (\pi - \theta_m) \theta_m}{(\pi - \theta_m)^2 - \sin^2 \theta_m}. \end{aligned} \right\} \quad (3.31)$$

It should be noted that from (3.9) and (3.22) the tangential components of \mathbf{u}_{A0} and \mathbf{u}_{B0} at the liquid interface both tend to zero as $r \rightarrow 0$. From the above solution (3.31) the asymptotic value of σ for $r \rightarrow 0$ may be calculated using (3.15) and (3.24) as

$$\sigma \sim \sigma_m + Ca [h(\theta_m) \ln r + P_0^* + \dots] + \dots, \quad (3.32)$$

where the function $h(\theta)$ is

$$h(\theta) \equiv -2 \left[\frac{\lambda \{(\pi - \theta) \cos \theta + \sin \theta\}}{(\pi - \theta)^2 - \sin^2 \theta} + \frac{\theta \cos \theta - \sin \theta}{\theta^2 - \sin^2 \theta} \right]. \quad (3.33)$$

The quantity P_0^* appearing in (3.32) is a constant of integration. Its value may be obtained by solving for σ in the outer region having prescribed, for example, the value of the interfacial tension σ at some fixed point in the outer region or the total amount of surfactant present on the liquid-liquid interface. The shape of the liquid-liquid interface for $r \rightarrow 0$ correct to order Ca^{+1} may be obtained by first deriving the normal stresses at the interface due to \mathbf{u}_0 and substituting into (3.26) and then solving for the interface shape making use of (3.27). In this process we take (see Cox 1986) the interface shape $f_0 + Caf_1 = 0$ to have the same contact line as $f_1 = 0$. Then for $r \rightarrow 0$, we obtain,

$$\theta \sim \{\theta_m + O(r)\} + Ca \sigma_m^{-1} \{f(\theta_m) \ln r + Q_0^* + \dots\} + \dots, \quad (3.34)$$

where

$$f(\theta) \equiv 2 \sin \theta \left\{ \frac{\lambda(\pi - \theta)}{(\pi - \theta)^2 - \sin^2 \theta} + \frac{\theta}{\theta^2 - \sin^2 \theta} \right\}, \quad (3.35)$$

and where Q_0^* , like P_0^* depends on λ, θ_m and the geometry involved in this outer region. In the procedure of matching this outer region solution onto a solution valid close to the contact line, it will be found (§5) that the value of the as yet unknown constant θ_m is a function of Ca and may be expanded as

$$\theta_m = \theta_{m0} + Ca \theta_{m1} + \dots \quad (3.36)$$

so that the asymptotic form (3.34) may be written as

$$\theta = \{\theta_{m0} + \dots\} + Ca \{f(\theta_{m0}) \ln r + Q_0^* + \theta_{m1} + \dots\} + \dots \quad (3.37)$$

4. Inner region

An inner region of expansion, valid close to the contact line, is defined (see Cox 1986) using variables made dimensionless by the quantities s , U and μ_A . We thus use polar coordinates (\hat{r}, ϕ) (with origin at the actual contact line) as independent variables where

$$\hat{r} \sim \epsilon^{-1}r \quad \text{as } \hat{r} \rightarrow \infty. \quad (4.1)$$

In this region, the velocity fields \mathbf{u}_A and \mathbf{u}_B , the interface slope angle $\theta = \theta(\hat{r})$ and the interfacial tension $\sigma = \sigma(\hat{r})$ are expanded as

$$\mathbf{u}_A = \hat{\mathbf{u}}_{A0} + O(Ca), \quad \mathbf{u}_B = \hat{\mathbf{u}}_{B0} + O(Ca), \quad (4.2)$$

$$\theta = \hat{\theta}_0(\hat{r}) + Ca \hat{\theta}_1(\hat{r}) + \dots, \quad (4.3)$$

$$\sigma = \hat{\sigma}_0(\hat{r}) + Ca \hat{\sigma}_1(\hat{r}) + \dots \quad (4.4)$$

We now express all the equations and boundary conditions for \mathbf{u}_A , \mathbf{u}_B , σ etc stated in §3 (with the tangential velocity satisfying the given slip boundary condition) in terms of the inner variables and substitute into the resulting equations the expansions (4.2), (4.3) and (4.4). The tangential stress and normal stress boundary conditions (3.4) and (3.5) on the liquid–liquid interface at order Ca^0 thus give

$$\hat{\sigma}_0 = \sigma_w, \quad (4.5)$$

$$\hat{\theta}_0 = \theta_w + O(\epsilon), \quad (4.6)$$

where σ_w and θ_w are constants of integration. If the configuration of the liquid–liquid interface is time-dependent, it may be shown [Cox 1986] that if (3.28) is satisfied, this unsteadiness is negligible in the inner region and one may take zero normal velocity as the kinematic boundary condition on the interface. Since the solution for the flow fields $\hat{\mathbf{u}}_{A0}$ and $\hat{\mathbf{u}}_{B0}$ will depend on the particular slip model which is used, we will not perform the detailed calculation of their values. Instead we will derive only the asymptotic form of the solution for $\hat{r} \rightarrow \infty$, since it is this which is required for the matching procedure. For such large values of \hat{r} , the boundary condition on the solid surface must approach the no-slip boundary condition. Then by solving for $\hat{\mathbf{u}}_{A0}$ and $\hat{\mathbf{u}}_{B0}$, we may determine the stress on the liquid–liquid interface. This may then be used in conjunction with the boundary conditions (3.4) and (3.5) to determine $\hat{\theta}_1$ and $\hat{\sigma}_1$ which then gives the surface-tension variation and interface shape for $\hat{r} \rightarrow \infty$ as

$$\sigma \sim \sigma_w + Ca [h(\theta_w) \ln \hat{r} + P_1^* + \dots] + \dots, \quad (4.7)$$

$$\theta \sim [\theta_w + O(\epsilon)] + Ca \sigma_w^{-1} [f(\theta_w) \ln \hat{r} + Q_1^* + \dots] + \dots \quad (4.8)$$

The arbitrariness of the integration constants P_1^* and Q_1^* in these results may be removed by defining σ_w and θ_w as the values taken at the solid boundary at $\hat{r} = 0$. These quantities P_1^* and Q_1^* will depend on λ , θ_w and the particular slip model which has been used. We expect θ_w , the contact angle at the solid surface, which we will call the *microscopic* contact angle, to have a value determined by the intermolecular forces acting very near the contact line. It will thus depend on not only the two liquid phases and the solid phase present, but also upon the concentration c_w of the surfactant present at the contact line. Thus we can expect θ_w to depend on the value of σ_w (which is related to c_w by (3.6)). It is not known, however, whether, in addition to this dependence on σ_w , the microscopic contact angle θ_w depends directly on the spreading velocity U . Indeed some authors (Cherry & Holmes 1969; Blake & Haynes 1969) have suggested that θ_w might depend on U even in the absence of a surfactant.

5. Matching with two and three regions

When the parameter ϵ is kept fixed and small while $Ca \rightarrow 0$, the expansion (3.34) for θ [and (3.32) for σ] valid in the outer region for $r \rightarrow 0$ may be matched onto the expansion (4.8) for θ (and (4.7) for σ) valid in the inner region for $\hat{r} \rightarrow \infty$. Then in a manner similar to that of Cox (1986), Huh & Mason (1977) and Hocking (1977) for a surfactant-free situation, we obtain values of σ_m and θ_m as

$$\sigma_m = \sigma_w + Ca \{h(\theta_w) \ln \epsilon^{-1} + P_i^* - P_0^*\}, \quad (5.1)$$

$$\theta_m = \theta_w + Ca \sigma_w^{-1} \{f(\theta_w) \ln \epsilon^{-1} + Q_i^* - Q_0^*\}. \quad (5.2)$$

Equation (5.1) relates the interfacial tension σ_w at the contact line to the spreading velocity U (involved in the definition of Ca) and to the interfacial tension σ_m . This quantity σ_m is the constant interfacial tension (which may depend on time t) in the outer region for $Ca = 0$ and is determined by the given total amount of surfactant present on the interface. Equation (5.2) relates the macroscopic contact angle θ_m determining the outer solution, to the spreading velocity U and to the microscopic contact angle θ_w . As already pointed out θ_w itself may be dependent on σ_w determined from (5.1). At any particular instant during the motion of the system, the macroscopic contact angle θ_m may be considered as the angle between the static interface shape $f_0 = 0$ and the solid surface at the contact line in the *outer* region. Or alternatively, it may be considered as being determined by the asymptotic form (3.42) of the interface shape in the outer region as the contact line is approached.

In a manner similar to that for the surfactant-free situation, (Cox 1986), it is seen that the results (5.1) and (5.2) are only valid for $Ca \rightarrow 0$, $\epsilon \rightarrow 0$ if the quantity $Ca \ln \epsilon^{-1}$ also tends to zero. Under such a situation, the liquid-liquid interface is approximately planar (with the interfacial tension approximately constant) near the contact line.

When $Ca \rightarrow 0$, $\epsilon \rightarrow 0$ with $Ca \ln \epsilon^{-1}$ of order unity, the results (5.1) and (5.2) are no longer valid since there is then no overlap of the inner and outer regions. It is then necessary to introduce a third region called the *intermediate* region which must exist between the inner and outer regions. This was done by Cox (1986) and Hocking & Rivers (1982) for the surfactant-free situation. In the subsequent discussion we limit ourselves to this situation $Ca \rightarrow 0$, $\epsilon \rightarrow 0$ with $\eta \equiv Ca \ln \epsilon^{-1}$ of order unity and thus make an expansion in Ca taking the parameter η fixed and of order unity.

6. Intermediate region

In the same manner as for the surfactant-free situation (Cox 1986), we use in the intermediate region, coordinates (\tilde{x}, ϕ) where \tilde{x} is defined by

$$\tilde{x} = Ca \ln \epsilon \hat{r}, \quad (6.1)$$

where

$$-\eta < \tilde{x} < 0. \quad (6.2)$$

Then it is seen that the end-points $\tilde{x} = 0$ and $\tilde{x} = -\eta$ correspond respectively to the outer region (with r of order unity) and the inner region (with \hat{r} of order unity). Thus the intermediate region expansion must be matched onto the outer region at $\tilde{x} = 0$ and onto the inner region at $\tilde{x} = -\eta$.

Since for any fixed value of $\tilde{x} < 0$, r is exponentially small for $Ca \rightarrow 0$, the flow is two-dimensional and so a stream function ψ may be defined which we will take to have the form

$$\psi = r\tilde{g}(\tilde{x}, \phi; \eta, Ca), \quad (6.3)$$

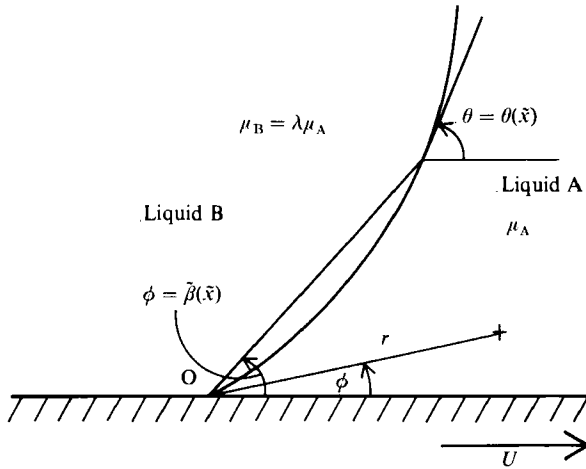


FIGURE 1. Intermediate region: coordinates are (\tilde{x}, ϕ) where $\tilde{x} = Ca \ln \epsilon^{\tilde{r}}$. Interface is $\phi = \tilde{\beta}(\tilde{x})$ and has slope $\theta = \theta(\tilde{x})$.

with corresponding pressure field

$$p_A = r^{-1} \tilde{h}_A(\tilde{x}, \phi; \eta, Ca), \tag{6.4}$$

in liquid A and

$$p_B = r^{-1} \lambda \tilde{h}_B(x, \phi; \eta, Ca), \tag{6.5}$$

in liquid B. The liquid–liquid interface is taken to be

$$\phi = \tilde{\beta}(\tilde{x}; \eta, Ca) \tag{6.6}$$

so that the angle θ its tangent makes with the solid surface (see figure 1) at any position is

$$\theta = \tilde{\beta} + \tan^{-1} \left(r \frac{d\phi}{dr} \right) = \tilde{\beta} + \tan^{-1} \left(Ca \frac{d\tilde{\beta}}{d\tilde{x}} \right). \tag{6.7}$$

From the form (6.3) of the stream function, the radial component u_r and transverse component u_ϕ of the velocity field in either liquid are

$$u_r = \frac{\partial \tilde{g}}{\partial \phi}, \quad u_\phi = -g - Ca \frac{\partial \tilde{g}}{\partial \tilde{x}}, \tag{6.8}$$

where, since ψ satisfies the biharmonic equation, \tilde{g} satisfies

$$\left(\frac{\partial^2}{\partial \phi^2} + 1 \right)^2 \tilde{g} = 2Ca^2 \frac{\partial^2}{\partial \tilde{x}^2} \left(1 - \frac{\partial^2}{\partial \phi^2} \right) \tilde{g} - Ca^4 \frac{\partial^4 \tilde{g}}{\partial \tilde{x}^4}. \tag{6.9}$$

As shown by Cox (1986) the given slip boundary condition on the solid surface may be replaced by the no-slip boundary condition, the error produced by this procedure being exponentially small as $Ca \rightarrow 0$. Thus at the solid surface the no-slip boundary condition may be written as

$$\tilde{g}_A = 0, \quad \frac{\partial \tilde{g}_A}{\partial \phi} = +1 \quad \text{on } \phi = 0, \tag{6.10}$$

$$\tilde{g}_B = 0, \quad \frac{\partial \tilde{g}_B}{\partial \phi} = -1 \quad \text{on } \phi = \pi. \tag{6.11}$$

If the liquid-liquid interface configuration is time dependent, it may be shown (Cox 1986) that so long as (3.28) is satisfied, the effect of such unsteadiness is exponentially small as $Ca \rightarrow 0$. Thus the normal component of velocity may be taken to be zero at the interface giving (Cox 1986)

$$\tilde{g}_A = \tilde{g}_B = 0 \quad \text{on } \phi = \tilde{\beta}, \tag{6.12}$$

this being correct to all orders in Ca . In our intermediate variables, the equation (3.7) with boundary condition (3.9) gives the tangential component of velocity on the interface as zero for both liquids. Then using the results given by Cox (1986), it is seen that this gives

$$\frac{\partial \tilde{g}_A^2}{\partial \phi} = \frac{\partial \tilde{g}_B^2}{\partial \phi} = 0 \quad \text{on } \phi = \tilde{\beta}, \tag{6.13}$$

correct to all orders in Ca . The tangential and normal-stress boundary conditions (using results obtained by Cox 1986) are likewise found to be respectively

$$\frac{d\sigma}{d\tilde{x}} = \left(\frac{\partial^2 \tilde{g}_A}{\partial \phi^2} - \lambda \frac{\partial^2 \tilde{g}_B}{\partial \phi^2} \right) + O(Ca^2) \quad \text{on } \phi = \tilde{\beta}, \tag{6.14}$$

and
$$\frac{d\tilde{\beta}}{d\tilde{x}} = \sigma^{-1} \left\{ \left(\frac{\partial \tilde{g}_A}{\partial \phi} + \frac{\partial^3 \tilde{g}_A}{\partial \phi^3} \right) - \lambda \left(\frac{\partial \tilde{g}_B}{\partial \phi} + \frac{\partial^3 \tilde{g}_B}{\partial \phi^3} \right) \right\} + O(Ca^2) \quad \text{on } \phi = \tilde{\beta}. \tag{6.15}$$

7. General solution

Since the equations (6.9) and the boundary conditions (6.10), (6.11), (6.12) and (6.13) for \tilde{g}_A and \tilde{g}_B (determining the flow field) contain no term of order Ca^{+1} , it follows that for small Ca

$$\tilde{g}_A = \tilde{g}_{A0} + O(Ca^2), \quad \tilde{g}_B = \tilde{g}_{B0} + O(Ca^2). \tag{7.1}$$

Substituting these expansions into (6.9) and boundary conditions (6.10)–(6.13) and equating terms in Ca^0 we obtain equations for \tilde{g}_{A0} , \tilde{g}_{B0} which possess the solution

$$\tilde{g}_{A0} = (C_A \phi + D_A) \cos \phi + (E_A \phi + F_A) \sin \phi, \tag{7.2}$$

$$\tilde{g}_{B0} = (C_B \phi + D_B) \cos \phi + (E_B \phi + F_B) \sin \phi, \tag{7.3}$$

where C_A, D_A, \dots are given by (3.31) with $\tilde{\beta}$ replacing θ_m . The equation (6.14) for the interfacial tension σ and the equation (6.15) for the interface shape with these values of \tilde{g}_A and \tilde{g}_B may then be solved to give

$$\sigma = (K_1 + Ca K_2) q(\tilde{\beta}) + O(Ca^2), \tag{7.4}$$

$$\tilde{x} = (K_1 + Ca K_2) g(\tilde{\beta}) + (K_3 + Ca K_4) + O(Ca^2), \tag{7.5}$$

where $(K_1 + Ca K_2)$ and $(K_3 + Ca K_4)$ are constants of integration which have been expanded for small Ca . The functions $q(\tilde{\beta})$ and $g(\tilde{\beta})$ are

$$q(\tilde{\beta}) = \exp \left[\int_0^{\tilde{\beta}} \frac{h(\beta)}{f(\beta)} d\beta \right], \tag{7.6}$$

$$g(\tilde{\beta}) = \int_0^{\tilde{\beta}} \frac{q(\beta)}{f(\beta)} d\beta. \tag{7.7}$$

Using (6.7), we may write (7.4) and (7.5) in the alternative form

$$\sigma = K_1 q(\theta) + Ca \{ K_2 q(\theta) - h(\theta) \} + O(Ca^2), \tag{7.8}$$

$$\tilde{x} = \{ K_1 g(\theta) + K_3 \} + Ca \{ K_2 g(\theta) - 1 + K_4 \} + O(Ca^2). \tag{7.9}$$

If this is matched at $\tilde{x} = 0$ onto the asymptotic forms (3.32) and (3.34) of the outer region solution for $r \rightarrow 0$, the values of the constants K_1 , K_2 , K_3 and K_4 may be obtained. These, when substituted back into (7.8) and (7.9), yield

$$\sigma = \frac{\sigma_m q(\theta)}{q(\theta_m)} + Ca \left[\frac{q(\theta)}{q(\theta_m)} \left\{ P_o^* - \frac{Q_o^* h(\theta_m)}{f(\theta_m)} + h(\theta_m) \right\} - h(\theta) \right] + O(Ca^2), \quad (7.10)$$

$$\begin{aligned} \tilde{x} = & \frac{\sigma_m}{q(\theta_m)} \{g(\theta) - g(\theta_m)\} \\ & + Ca \left[\frac{\{g(\theta) - g(\theta_m)\}}{q(\theta_m)} \left\{ P_o^* - \frac{Q_o^* h(\theta_m)}{f(\theta_m)} + h(\theta_m) \right\} - \frac{Q_o^*}{f(\theta_m)} \right] + O(Ca^2). \end{aligned} \quad (7.11)$$

If these solutions are now matched at $\tilde{x} = -\eta$ onto the asymptotic forms (4.7) and (4.8) of the inner-region solution for $\hat{r} \rightarrow \infty$, we obtain

$$\begin{aligned} \sigma_w = & \frac{q(\theta_w)}{q(\theta_m)} \left[\sigma_m + Ca \left\{ -\frac{q(\theta_m)}{q(\theta_w)} P_i^* + P_o^* + \frac{q(\theta_m) h(\theta_w)}{q(\theta_w) f(\theta_w)} Q_i^* \right. \right. \\ & \left. \left. - \frac{h(\theta_m)}{f(\theta_m)} Q_o^* + h(\theta_m) - \frac{q(\theta_m) h(\theta_w)}{q(\theta_w)} \right\} + O(Ca^2) \right], \end{aligned} \quad (7.12)$$

and

$$\begin{aligned} Ca = & \frac{\sigma_m \{g(\theta_m) - g(\theta_w)\}}{q(\theta_m)} \left[\ln(\epsilon^{-1}) + \frac{Q_i^*}{f(\theta_w)} - \frac{Q_o^*}{f(\theta_m)} + \frac{\{g(\theta_m) - g(\theta_w)\}}{q(\theta_m)} \right. \\ & \left. \times \left\{ \frac{h(\theta_m)}{f(\theta_m)} Q_o^* - P_o^* - h(\theta_m) \right\} \right]^{-1} + O\left(\frac{1}{\ln(\epsilon^{-1})}\right)^2, \end{aligned} \quad (7.13)$$

where use has been made of the assumption that η is of order unity. If liquid A is receding so that $U < 0$, these results are still valid [as are also the definitions of P_i^* , P_o^* , Q_i^* , and Q_o^* given by (4.7), (3.32), (4.8), and (3.37)] if $Ca \equiv \mu_A U/\sigma$ is taken as being negative. In the results (7.12) and (7.13), it should be remembered that the quantities P_i^* and Q_i^* , obtained from the inner-region solution, depend on θ_w and P_o^* and Q_o^* , obtained from the outer region solution, depend on θ_m . Thus if θ_m , θ_w and σ_m are known, (7.13) will determine the value of Ca and hence the spreading velocity U . Then with this value of Ca , (7.12) will determine the value of σ_w .

Rather than θ_m , θ_w , and σ_m being known, a more usual situation is one in which only U and σ_m are known. This will occur whenever the contact line is forced to move with a velocity U and the total interface area is a constant in time with a known amount of surfactant present determining σ_m (as for a meniscus forced to move along a tube with speed U). Then θ_m , θ_w , and σ_w are determined by (7.12), (7.13), and the relation

$$\theta_w = \theta_w(\sigma_w), \quad (7.14)$$

mentioned in §4, between the microscope contact angle θ_w and the interfacial tension σ_w (or the surfactant concentration c_w) of the interface at the wall.

A more complicated situation may occur in which the spreading speed U is unknown and the total interface area A may vary in time. Such is the situation for a drop spreading on a plane surface (which for the surfactant-free situation was solved by Hocking & Rivers 1982). Then U , θ_m , θ_w , σ_m , and σ_w are determined by (7.12), (7.13), and (7.14) together with (i) a relation between σ_m and A (obtained by eliminating c_m from (3.6) and the surfactant conservation equation (3.20)) and (ii) a supplementary equation such as conservation of liquid volume (for a drop spreading

on a plane surface) or a given value of the pressure drop across the interface (for a meniscus moving along a non-uniform tube with a given pressure drop across the interface).

When no surfactant is deposited on the solid surface (assumption (c) of §2), the explicit form of (7.14) may be obtained by noting that if the contact line is moved a distance dl (from liquid A to liquid B) at an infinitesimally small speed, conservation of energy yields

$$(\sigma_B - \sigma_A) dl = \sigma_w \cos \theta_w dl, \quad (7.15)$$

if the interfacial tension of the surfactant-covered interface is σ_w . In (7.15), σ_A and σ_B are the surface energies per unit area of the solid surface in contact with the liquid A and with the liquid B respectively. If the microscopic contact angle of the surfactant-free interface is θ_0 , then a similar argument applied to such an interface gives

$$(\sigma_B - \sigma_A) dl = \sigma_0 \cos \theta_0 dl, \quad (7.16)$$

where σ_0 is the interfacial tension of the surfactant-free interface. From (7.15) and (7.16) we obtain the relation (7.14) as

$$\cos \theta_w = \frac{\sigma_0}{\sigma_w} \cos \theta_0. \quad (7.17)$$

This gives a real value for θ_w only if

$$\sigma_w \geq \sigma_0 |\cos \theta_0|, \quad (7.18)$$

so that the interfacial tension at the wall must not fall below $\sigma_0 |\cos \theta_0|$.

8. Discussion

It may readily be shown that up to and including terms of order Ca^{+1} , the results (7.12) and (7.13) obtained from the triple-region expansion procedure reduce to the results (5.1) and (5.2) obtained from the double-region expansion procedure under the conditions when the latter is valid (i.e. when $Ca \ln(\epsilon^{-1}) \rightarrow 0$ as $Ca \rightarrow 0$, $\epsilon \rightarrow 0$). However the two sets of results are distinct when $Ca \ln(\epsilon^{-1})$ is of order unity as $Ca \rightarrow 0$, $\epsilon \rightarrow 0$, the results (5.1) and (5.2) then no longer being valid.

At lowest order in Ca , the results (7.12) and (7.13) reduce to

$$\sigma_w = \frac{q(\theta_w)}{q(\theta_m)} \sigma_m + O(Ca), \quad (8.1)$$

$$\frac{\sigma_m}{q(\theta_m)} \{g(\theta_m) - g(\theta_w)\} = Ca \ln(\epsilon^{-1}) + O(Ca), \quad (8.2)$$

which have the advantage that they do not involve P_1^* , P_0^* , Q_1^* , and Q_0^* and hence are independent of the geometry of the flow in the outer region and independent of the slip model chosen for the inner region. However, (8.1) and (8.2) do have the disadvantage that the parameter $\epsilon \equiv s/R$ which appears, does not have a unique value as neither the slip length s nor the macroscopic length R possess unique definitions. This non-uniqueness is eliminated if the terms of order Ca^{+1} are included (as in the original results (7.12) and (7.13)). The appearance of ϵ in (8.2) means that by merely changing the macroscopic lengthscale R , keeping θ_w , σ_m , and Ca fixed, the value of the macroscopic contact angle θ_m and the variation of σ along the interface should be changed. The dependence of θ_m on R was also found for the movement of

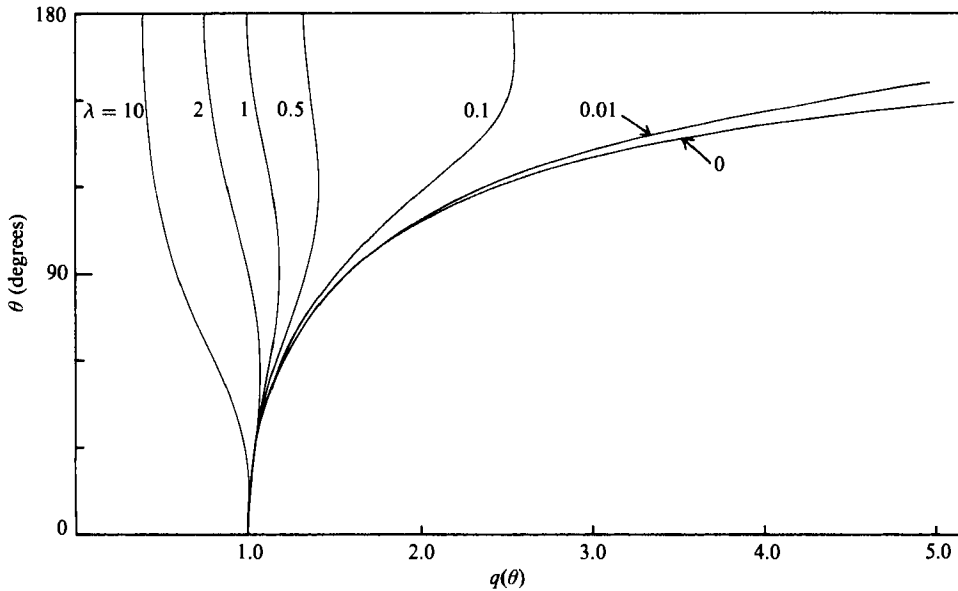


FIGURE 2. $q(\theta)$ for various values of λ .

a surfactant-free interface (Cox 1986) and has been demonstrated experimentally [Ngan & Dussan V. 1982] for that situation.

The function $q(\theta)$, given by (7.6), which describes the interfacial tension variation along the interface in the intermediate region (see (8.1)) has been plotted in figure 2 for various values of λ . It is seen that for all values of λ (except $\lambda = 0$ and $\lambda = \infty$) $q(\theta)$ increases with θ to a maximum value at $\theta = \theta^*$ and then decreases with θ , where θ^* and λ are related by $h(\theta^*) = 0$ or

$$\lambda = \frac{\{(\pi - \theta^*)^2 - \sin^2 \theta^*\} (\sin \theta^* - \theta^* \cos \theta^*)}{(\theta^{*2} - \sin^2 \theta^*) \{\sin \theta^* - (\pi - \theta^*) \cos \theta^*\}} \quad (8.3)$$

The function $g(\theta)$, given by (7.7) and involved in the relation (8.2) for the value of the macroscopic contact angle θ_m , is likewise plotted in figure 3 for various values of λ . These results are qualitatively similar to the results for the equivalent function applicable to a surfactant-free interface (Cox 1986) in that $g(\theta)$ attains a finite maximum value at $\theta = 180^\circ$ for all λ , except $\lambda = 0$ for which $g(\theta) \rightarrow \infty$ as $\theta \rightarrow 180^\circ$.

In order to compare the present results quantitatively with those for a surfactant-free interface (Cox 1986), the value of the macroscopic contact angle θ_m has been plotted in figure 4 as a function of $Ca \ln(\epsilon^{-1})$ for several values of λ for the surfactant present and for the surfactant absent for θ_w fixed (and equal to 40°). It is observed that for λ close to unity the surfactant has little effect but that there can be a large effect for λ either small or large. However such results, for when the surfactant is present, are not realistic since θ_w cannot really be considered fixed and should be considered as a function of σ_w . Thus assuming the relation (7.17) between θ_w and σ_w the results (8.1) and (8.2) may be used to calculate the macroscopic contact angle as a function of $Ca \ln(\epsilon^{-1})$ [and hence of the spreading velocity U] for any chosen value of σ_m (determined by the surfactant concentration in the outer region) and λ . The characteristic interfacial tension σ^* used to make quantities dimensionless may be chosen as the magnitude of the difference in the surface energies per unit area of the solid surface in contact with the liquid A and with the liquid B, so that either

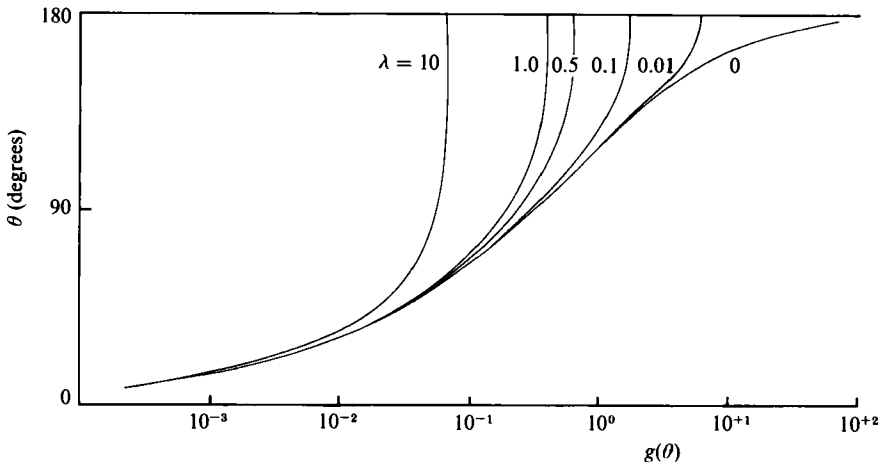


FIGURE 3. $g(\theta)$ for various values of λ .

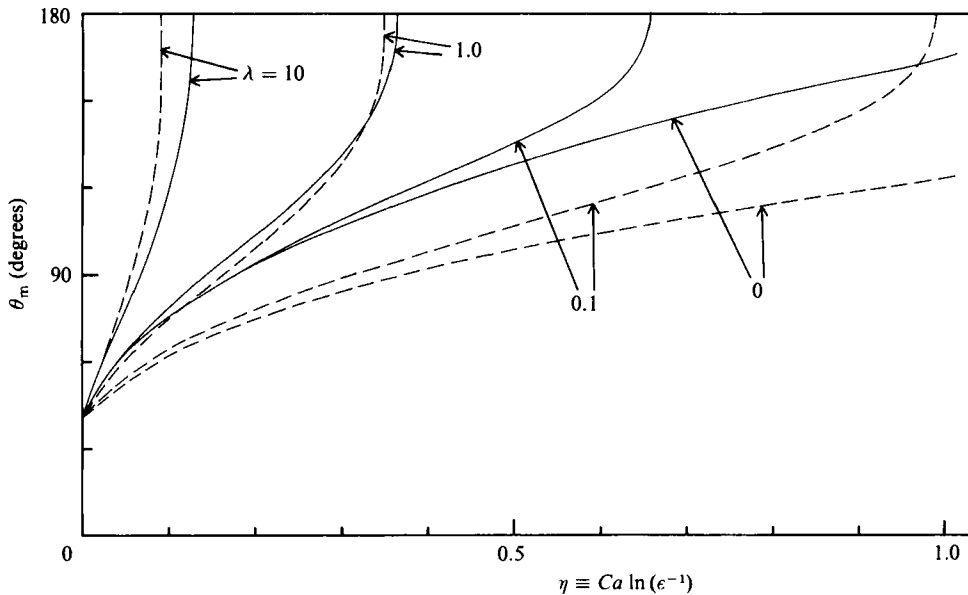


FIGURE 4. Macroscopic contact angle θ_m as a function of $Ca \ln(\epsilon^{-1})$ for various values of λ with $\theta_w = 40^\circ$. Continuous lines are the results obtained from the present theory whilst the broken lines are for a surfactant-free interface (Cox 1986).

$\sigma_0 \cos \theta_0 = +1$ (for $\theta_w < 90^\circ$) or $\sigma_0 \cos \theta_0 = -1$ (for $\theta_w > 90^\circ$). Depending on the values of σ_m and λ (and on whether $\sigma_0 \cos \theta_0$ was $+1$ or -1) it was found that many different types of behaviour could occur. The results for 11 particular examples (cases A–L) are shown in figure 5(a, b, c) in which values of θ_m and θ_w have been plotted as a function of $\eta \equiv Ca \ln(\epsilon^{-1})$ for cases A–F and as a function of $\eta_B \equiv (\mu_B U/\sigma^*) \ln(\epsilon^{-1})$ for cases G–L. The corresponding values of σ_m , σ_w and the maximum value σ_{max} of σ (if different from σ_m or σ_w) are plotted in figure 6(a, b, c). It is observed that as Ca is increased, a solution may fail to exist at some critical Ca due to $\theta_m \rightarrow 180^\circ$ (cases B, C, E, and F) or due to $\theta_w \rightarrow 0^\circ$ (case D). In case F, both θ_m and $\theta_w \rightarrow 180^\circ$ at this critical Ca . Case A is interesting in that the solution fails

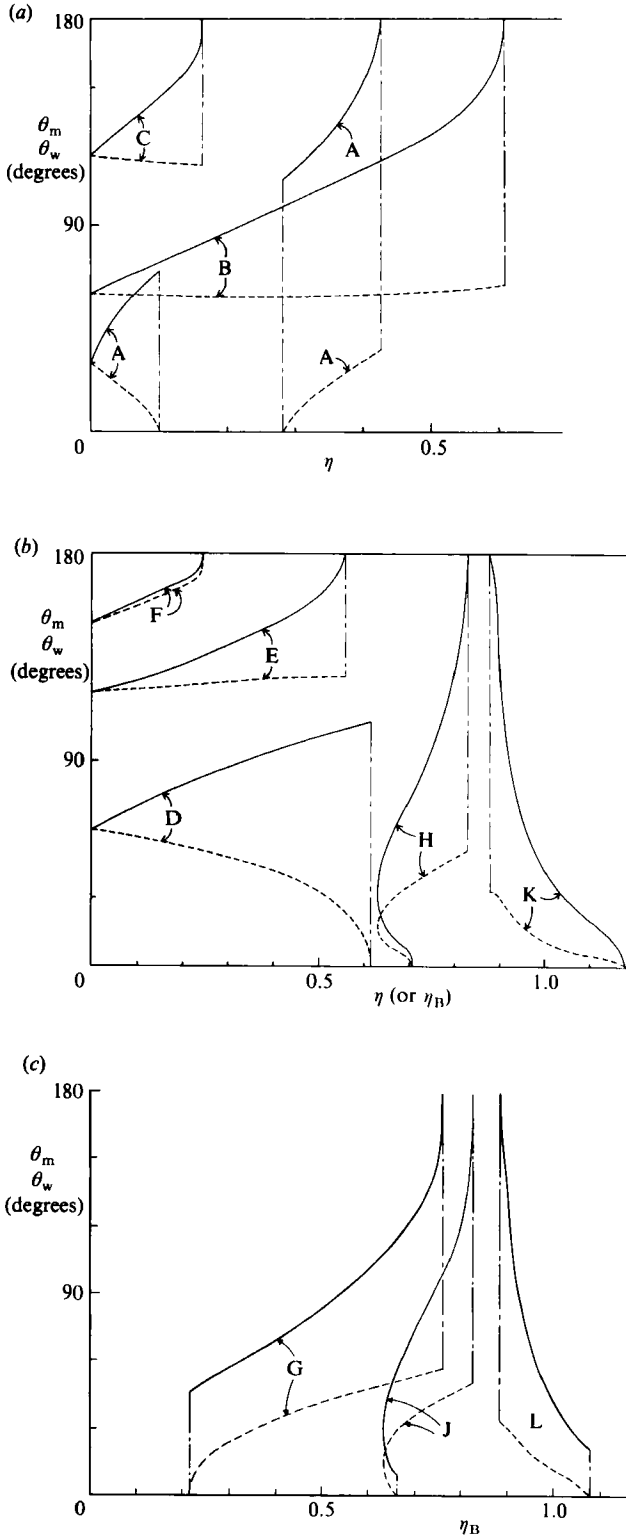


FIGURE 5(a-c). For caption see facing page.

to exist at $Ca \ln(\epsilon^{-1}) \simeq 0.10$ due to $\theta_w \rightarrow 0^\circ$ but then exists again at $Ca \ln(\epsilon^{-1}) \simeq 0.28$ (with $\theta_w = 0^\circ$) up to $Ca \ln(\epsilon^{-1}) \simeq 0.43$ where the solution again fails to exist but this time because $\theta_m \rightarrow 180^\circ$. Since in the limit of no motion $Ca \rightarrow 0$, $\sigma_m = \sigma_w$ it follows from (7.18) that in this limit $\sigma_m \geq 1$. However solutions for $0 < \sigma_m < 1$ can exist for $Ca \neq 0$ (cases H, J, K and L). Thus for case H it is seen that above $\lambda Ca \ln(\epsilon^{-1}) \simeq 0.63$, two solutions exist, one of which has θ_m increasing with Ca (with $\theta_m \rightarrow 180^\circ$ at $\lambda Ca \ln(\epsilon^{-1}) \simeq 0.83$) while the other has θ_m decreasing with Ca (with $\theta_m \rightarrow 0^\circ$ at $\lambda Ca \ln(\epsilon^{-1}) \simeq 0.71$). For case K, just one solution exists for $0.88 < \lambda Ca \ln(\epsilon^{-1}) < 1.18$, with θ_m decreasing with Ca from a value of 180° at $\lambda Ca \ln(\epsilon^{-1}) = 0.88$ to 0° at $\lambda Ca \ln(\epsilon^{-1}) = 1.18$. Cases J and L are similar to H and K respectively except that θ_m does not tend to zero in the limiting situation $\theta_w \rightarrow 0^\circ$. The question arises as to which of the two solutions in case H (and J) would actually occur. This may depend on the previous history of the system or it may be that one solution is unstable. In fact the unusual situation where θ_m decreases with Ca (in cases H, J, K and L) may well be unstable since if a portion of the contact line near O (see figure 1) is displaced to the right of its true position at any instant, θ_m will usually be larger and so Ca (and hence the velocity of the contact line relative to the solid surface) will be reduced. This would cause the contact line to move still further ahead to the right. Thus disturbances to the contact line position will be amplified.

Since no solution for case H ($\lambda = \infty$, $\sigma_0 \cos \theta_0 = +1$, $\sigma_m = 0.55$) exists for $0 < \eta_B < 0.63$, the behaviour in this range of η_B is unknown so that it is uncertain whether case H for $\eta_B > 0.63$ (with θ_m increasing with Ca) can be reproduced by keeping σ_m fixed (and equal to 0.55) and increasing η_B from zero to beyond the value 0.63. However this case H can be obtained (see figure 7e with the roles of liquids A and B interchanged) by starting with $\sigma_m = 1.5$ at $\eta_B = 0$ (giving $\theta_m = \theta_w = 48.2^\circ$) and then increasing η_B to a value of 0.7 (for which $\theta_m \simeq 102^\circ$). Keeping the value of η_B now fixed at 0.7, the surfactant concentration far from the interface may be increased to reduce σ_m from 1.5 down to the required value of 0.55 (for which $\theta_m \approx 73^\circ$). In this manner the case H (with $0.63 < \eta_B < 0.83$) may be obtained in a continuous and predictable way. Similar remarks also apply to case J.

From figure 6(a, b, c) it is noted that the maximum value σ_{\max} of the interfacial tension σ can occur either at or near the inner region where $\sigma = \sigma_w$ (cases C, G, H, J, K and L) or at or near the outer region where $\sigma = \sigma_m$ (cases A, B, D, E and F) or at some fixed point in the middle of the intermediate region (cases A, B, and E), with the point at which this maximum value of σ occurs being possibly dependent on the value of Ca . The minimum value of σ can only occur at the inner region (cases A, B, D, E and F) or at the outer region (cases A, B, C, G, H, J, K and L).

A very convenient way to show the results obtained from (7.17), (8.1), and (8.2) is to plot the macroscopic contact angle θ_m as a function of the interfacial tension

FIGURE 5. Values of θ_m (—) and θ_w (---) as a function of $\eta \equiv Ca \ln(\epsilon^{-1})$ [or of η_B for cases G, H, J, K, L] for case A: $\lambda = 1$, $\sigma_0 \cos \theta_0 = +1$, $\sigma_m = 1.1547$ (giving $\theta_m = \theta_w = 30^\circ$ at $Ca = 0$). B: $\lambda = 1$, $\sigma_0 \cos \theta_0 = +1$, $\sigma_m = 2$ (giving $\theta_m = \theta_w = 60^\circ$ at $Ca = 0$). C: $\lambda = 1$, $\sigma_0 \cos \theta_0 = -1$, $\sigma_m = 2$ (giving $\theta_m = \theta_w = 120^\circ$ at $Ca = 0$). D: $\lambda = 0$, $\sigma_0 \cos \theta_0 = +1$, $\sigma_m = 2$ (giving $\theta_m = \theta_w = 60^\circ$ at $Ca = 0$). E: $\lambda = 0.1$, $\sigma_0 \cos \theta_0 = -1$, $\sigma_m = 2$ (giving $\theta_m = \theta_w = 120^\circ$ at $Ca = 0$). F: $\lambda = 0$, $\sigma_0 \cos \theta_0 = -1$, $\sigma_m = 1.1547$ (giving $\theta_m = \theta_w = 150^\circ$ at $Ca = 0$). G: $\lambda = 10$, $\sigma_0 \cos \theta_0 = +1$, $\sigma_m = 0.9$ (no solution for $Ca = 0$). H: $\lambda = \infty$, $\sigma_0 \cos \theta_0 = +1$, $\sigma_m = 0.55$ (no solution for $Ca = 0$). J: $\lambda = 10^4$, $\sigma_0 \cos \theta_0 = +1$, $\sigma_m = 0.55$ (no solution for $Ca = 0$). K: $\lambda = \infty$, $\sigma_0 \cos \theta_0 = +1$, $\sigma_m = 0.25$ (no solution for $Ca = 0$). L: $\lambda = 10^4$, $\sigma_0 \cos \theta_0 = +1$, $\sigma_m = 0.25$ (no solution for $Ca = 0$). Note: In order to conveniently plot the results, we have for the cases G–L plotted quantities as a function of $\eta_B \equiv (\mu_B U/\sigma^*) \ln(\epsilon^{-1})$ instead of as a function of η .

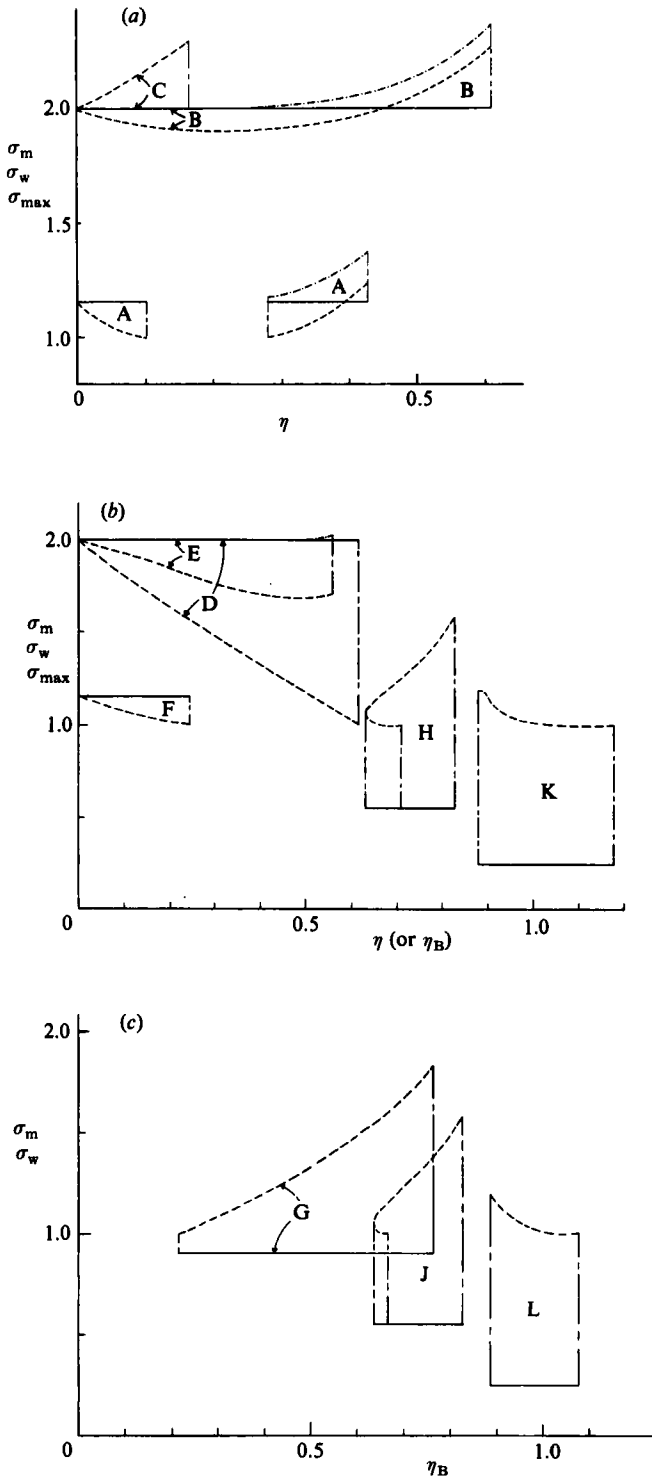


FIGURE 6. Values of σ_m (—), σ_w (---) and σ_{max} (-.-.-) as a function of η [or of η_B for cases G, H, J, K, L] for each of the cases represented in figure 5 (a-c).

σ_m for a fixed value of λ (and $\sigma_0 \cos \theta_0$ equal to either $+1$ or -1) for various (positive and negative) values of η . In this manner the results from $\lambda = 0, 0.1, 1.0$ and 10.0 ($\sigma_0 \cos \theta_0 = +1$) and for $\lambda = 0$ ($\sigma_0 \cos \theta_0 = -1$) (which may be used for $\lambda = \infty$ ($\sigma_0 \cos \theta_0 = +1$) by interchanging the roles of the liquids A and B, replacing θ_m by $180^\circ - \theta_m$ and Ca by $-\mu_B U/\sigma^*$), are shown in figure 7(a-e). The broken lines in these figures show the limiting situation for a solution to exist (and corresponds to $\theta_w = 0^\circ$). From these results it is observed that for $\sigma_0 \cos \theta_0 = +1$, if $\lambda \leq 1$ solutions exist only for $\sigma_m \geq 1$, whilst if $\lambda > 1$ solutions exist for all $\sigma_m \geq$ some σ_m^* where $\sigma_m^* = q(\pi)$ and therefore lies between 0 and 1 and tends to 0 as $\lambda \rightarrow \infty$ (see figure 2). However for large λ and small values of $\sigma_m (> \sigma_m^*)$, the solution obtained may represent an unstable situation (cases K and L). It is also seen that whereas for the surfactant-free interface with $\lambda = 0$, solutions exist for all values of Ca however large [Cox 1986], this is not the case for the present situation in which no solutions exist above a critical $Ca \ln(\epsilon^{-1})$ due to $\theta_w \rightarrow 0$ (for $\sigma_0 \cos \theta_0 = +1$ with $Ca > 0$) or to $\theta_m \rightarrow 180^\circ$ (for $\sigma_0 \cos \theta_0 = -1$ with $Ca > 0$).

The general behaviour described above and illustrated in figures 5-7 can be given a physical interpretation by noting that liquid A in the intermediate region produces a shear stress on the interface (see (3.33)) of $2(\sin \theta - \theta \cos \theta)/(\theta^2 - \sin^2 \theta)$ which is a monotonically decreasing function of θ which $\sim 2\theta^{-1}$ as $\theta \rightarrow 0$ and $\rightarrow 2\pi^{-1}$ as $\theta \rightarrow \pi$. The same flow also produces a normal stress on the interface (see (3.35)) of $2\theta \sin \theta/(\theta^2 - \sin^2 \theta)$ which is also a monotonically decreasing function of θ which $\sim 6\theta^{-2}$ as $\theta \rightarrow 0$ and $\rightarrow 0$ as $\theta \rightarrow \pi$. Thus for cases A-J in which θ_m is predicted to increase with increasing Ca , the direction of the shear stress on the interface may be obtained (see table 1). From this, the behaviour for increasing Ca of the maximum interfacial tension σ_{\max} (if it exists) and of σ_w may be predicted from (3.4). Then (7.17) gives the behaviour of θ_w which together with the behaviour of the normal stress on the interface can then be sometimes used to predict the behaviour of θ_m with increasing Ca . Finally one can then predict whether the change in shape of the interface (due to increasing Ca) has the same effect on σ_{\max} and σ_w as that predicted above due to the direct effect of increasing Ca . All these results for each of the cases A-J for various ranges of η are tabulated in table 1. For cases H-L in which θ_m is predicted to be a decreasing function of Ca , since θ_w is small and hence σ_w is close to unity, a different approach is taken. Thus for such cases, $\sigma_w - \sigma_m$ does not change very much over the range of η for which a solution exists. For cases H and K for which $\lambda = \infty$, the normal stress on the interface tends to 0 and $\theta_w \rightarrow 0$. Hence $\theta_m \rightarrow 0$ as $\theta_w \rightarrow 0$. This implies that the dimensionless shear stress on the interface decreases as $\theta_w \rightarrow 0$, so that since $\sigma_w - \sigma_m$ does not change much, the equation (3.4) would imply that Ca must increase for $\theta_w \rightarrow 0$. This behaviour is indicated in table 2. A similar situation exists for cases J and L (λ large but not infinite) except that as $\theta_w \rightarrow 0$, the normal stress and θ_m decrease to small positive values (and not to zero) due to the normal stress caused by the motion of the liquid A.

If we omit the cases where θ_m is a decreasing function of Ca which as already indicated would seem to correspond to an unstable situation, it is seen that there are at least three ways in which a solution can fail to exist. These are:

(a) (Case A, $\eta > 0.42$, case B, $\eta > 0.61$; case C, $\eta > 0.17$; case E, $\eta > 0.56$; case G, $\eta_B > 0.76$; case H, $\eta_B > 0.83$; case J, $\eta_B > 0.83$.) In these situations $\theta_m = 180^\circ$ (with θ_w tending to a constant value $< 180^\circ$) indicating that if the limiting values of η are exceeded that the motion becomes unsteady with a thick layer of liquid B being drawn beneath liquid A by the solid (see figure 8) which may then break up into drops.

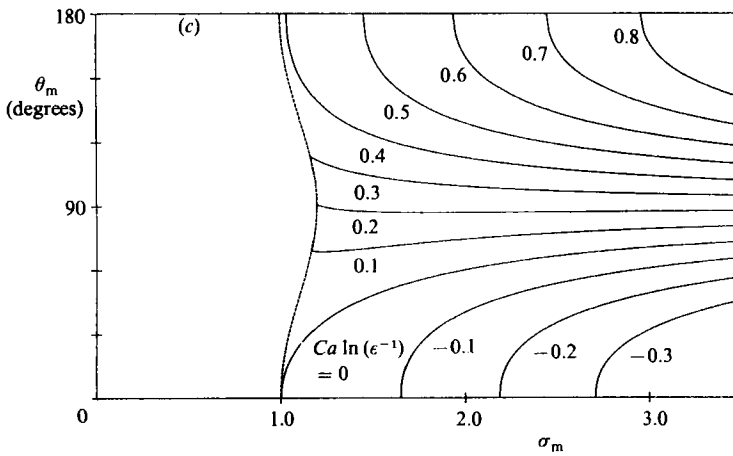
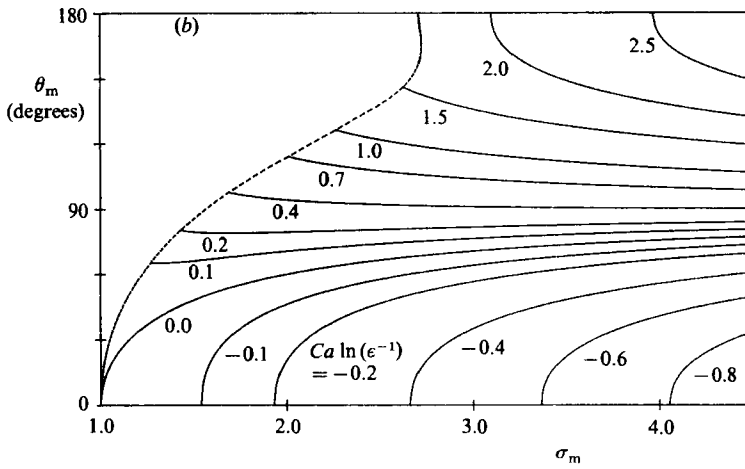
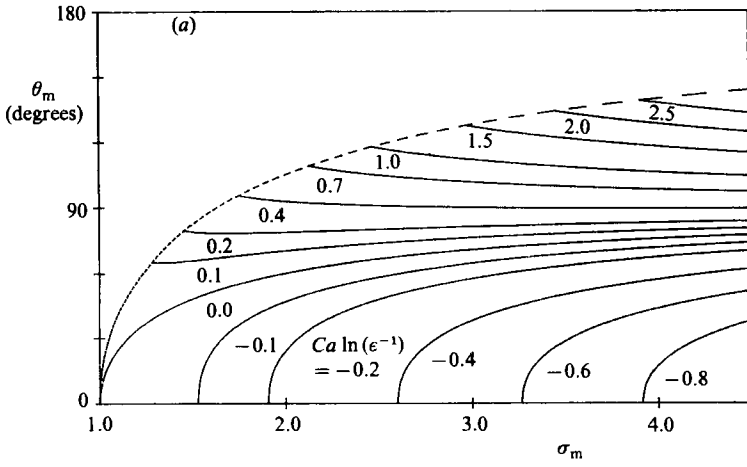


FIGURE 7(a-c). For caption see facing page.

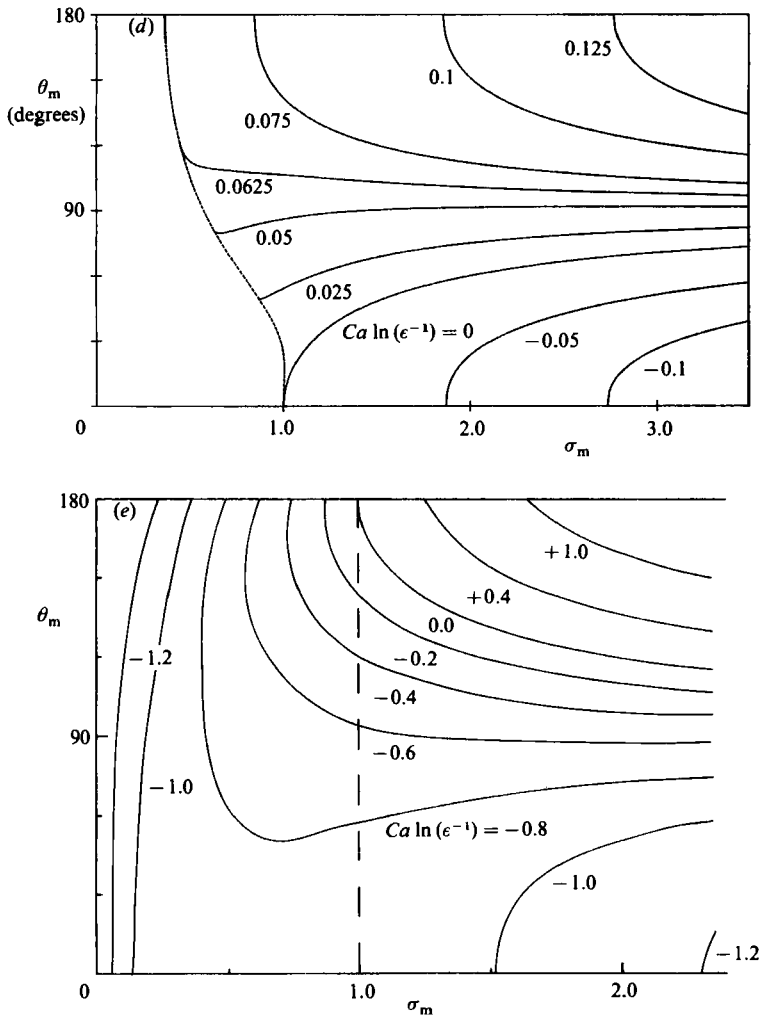


FIGURE 7. Values of θ_m as a function of σ_m for various values of $Ca \ln(\epsilon^{-1})$ for: (a) $\sigma_0 \cos \theta_0 = +1$, $\lambda = 0$; (b) $\sigma_0 \cos \theta_0 = +1$, $\lambda = 0.1$; (c) $\sigma_0 \cos \theta_0 = +1$, $\lambda = 1.0$; (d) $\sigma_0 \cos \theta_0 = +1$, $\lambda = 10.00$; (e) $\sigma_0 \cos \theta_0 = -1$, $\lambda = 0$. The broken line in each case is the limit ($\theta_w = 0$) for the existence of a solution.

(b) (Case A, $\eta > 0.1$ and $\eta < 0.28$; case D, $\eta > 0.62$; case G, $\eta_B < 0.22$). In these situations $\theta_w \rightarrow 0^\circ$ (with θ_m tending to a constant value $> 0^\circ$) and $\sigma_w \rightarrow +1$ indicating that beyond the limiting values of η a very thin film of surfactant-covered liquid A will spread from the contact line under liquid B against the motion of the solid surface (see figure 8). The mechanics of the motion of such a thin film would determine its length and should this be greater than s , then the flow in the intermediate region would be modified (since \mathbf{u}_B would be zero at the film).

(c) (Case F, $\eta > 0.24$). In this situation both θ_w and θ_m tend to 180° simultaneously with $\sigma_w \rightarrow +1$, indicating that if the limiting value of η is exceeded, a very thin film of surfactant-covered liquid B will spread from the contact line under liquid A and be carried downstream by the moving solid surface (see figure 8).

In addition to the above, it is possible with the correct combination of values for λ , $\sigma_0 \cos \theta_0$ and σ_m to have a situation (case intermediate between B and D) in which

Case	λ	$\sigma_0 \cos \theta_0$	σ_w	θ_w for $Ca = 0$	Range of γ	(a) Stress direction	(b) σ_{max}	(c)		(d) Effect of shape change	(e) Theory-breakdown type		
								σ_w	θ_m				
A	1.0	+1	1.155	30°	0-0.1 0.1	I I	x x	+	0°	?	(ii)		
												No solution	?
B	1.0	+1	2.0	60°	0-0.22 0.28-0.39 0.39-0.42 0.42	I, O I, O I, O I, O	✓ ↑ ↑ ✓	-	0°	↑ ↑ ↑ 180°	x ✓ — —		
												C	1.0
D	0.0	+1	2.0	60°	0-0.62 0.62	I I	x x	+	-	?	?		
												E	0.1
F	0.0	-1	1.15	150°	0-0.24 0.24	I I	x —	+	-	180°	↑ 180°		
												G	10
H	∞	+1	0.55	x	0.63-0.83 0.83	O —	x —	+	-	↑ 180°	— —		
												J	∞

TABLE 1. For all cases in which θ_m is an increasing function of Ca , this table gives for various ranges of γ : (a) Shear-stress direction on the interface [I, inwards towards the contact line; O, outwards away from the contact line; I, O, inwards near the contact line and outward farther from the contact line]. (b) Behaviour of σ_{max} : ✓, σ_{max} exists; x, σ_{max} does not exist; ↑, σ_{max} exists and is an increasing function of Ca . (c) Behaviour of σ_w , θ_w and θ_m as Ca is increased [↑, increases; ↓, decreases]. (d) Is the effect of interface shape change on σ qualitatively the same as the effect of increasing Ca ? ✓, yes, x, no]. (e) Type of theory breakdown (see figure 8). ?, situation where no conclusion can be drawn. (↑), actual results from figures 5, 6 indicate an increasing function of Ca (but not predictable by the present argument).

Case	λ	$\sigma_0 \cos \theta_0$	σ_w	θ_w for $Ca = 0$	Range of η	(a)			(b)			(c)
						Stress direction	Normal stress	θ_m	Shear stress	Ca	Theory-breakdown type (ii)?	
H	∞	+1	0.55	x	0-0.63	O	No solution	No solution	No solution	No solution	No solution	unstable?
K	10^4	+1	0.55	x	0.63-0.75 0.75	O	No solution	No solution	No solution	No solution	No solution	unstable?
J	10^4	+1	0.55	x	0-0.63	O	No solution	No solution	No solution	No solution	No solution	(ii)?
L	10^4	+1	0.55	x	0.63-0.66 0.66	O	No solution	No solution	No solution	No solution	No solution	unstable?

TABLE 2. For cases (H-L) in which θ_m is a decreasing function of Ca , this table gives for various ranges of η : (a) Shear-stress direction on the interface. O, outwards away from the contact line. (b) Behaviour of normal stress on the interface, of θ_m , of shear stress on the interface and of Ca as $\theta_w \rightarrow 0$. \uparrow , increases; \downarrow , decreases; $\rightarrow 0$, tends to zero. (c) Type of theory breakdown (see figure 8).

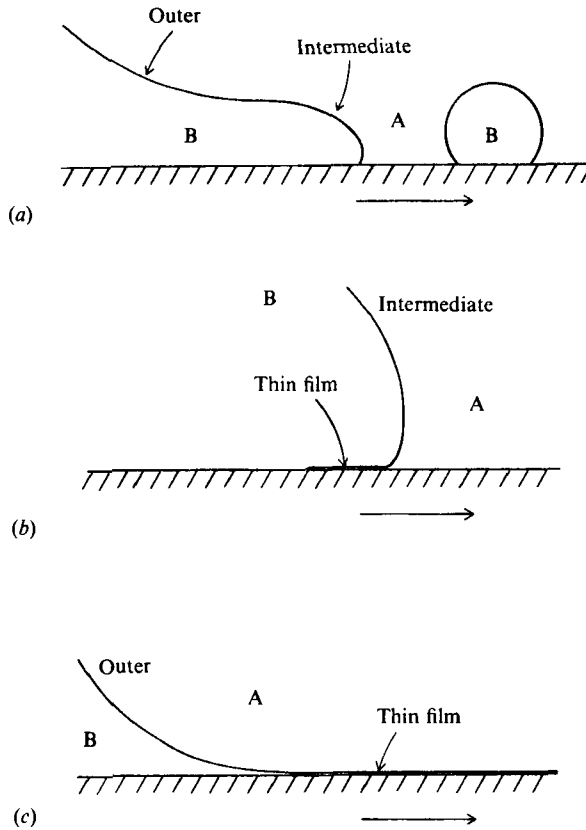


FIGURE 8. The ways in which a solution can fail to exist: (a) $\theta_m \rightarrow 180^\circ$ with $\theta_w < 180^\circ$. If critical η is exceeded, a layer of liquid B is pulled out which may then break up into drops. (b) $\theta_w \rightarrow 0^\circ$ with $\theta_m > 0^\circ$. If critical η is exceeded, a thin film of surfactant-covered liquid A spreads along the solid surface against its motion. (c) $\theta_w \rightarrow 180^\circ$ and $\theta_m \rightarrow 180^\circ$. If critical η is exceeded, a thin film of surfactant covered liquid B is carried along by the solid surface.

at a critical value of η , $\theta_w \rightarrow 0^\circ$ with $\theta_m \rightarrow 180^\circ$ [i.e. cases (a) and (b) above occur at the same critical η]. In such a situation a thick layer of liquid B would be pulled under fluid A in the direction of U while a thin film of liquid A would still exist between the layer of liquid A and the solid surface. The layer of liquid A may then break up into drops.

For cases H and J if η_B is decreased below the critical value for the solution to exist it is not clear what happens, although for sufficiently small η_B since σ_w would be less than unity, it would appear that the situation (b) described above would exist.

For the surfactant-free situation [Cox 1986] the solution can fail to exist only in the manner (a).

The conditions for the validity of the assumptions listed in §2 will now be discussed. If the surface (shear or dilational) viscosity of the interface is of order μ_s , then the maximum surface stress generated by the flow in any of the three expansion regions is of order $\mu_s U/R$. This is negligible [assumption (a)] and so surface rheology effects may be disregarded if

$$\frac{\mu_s U}{R\sigma^*} \equiv \frac{\mu_s}{\mu_A} Ca \ll 1. \quad (8.4)$$

The transport of surfactant in the liquids to or from the interface is diffusion dominated if

$$\frac{UR}{D_1} \ll 1, \quad (8.5)$$

where D_1 is the characteristic diffusion constant for the surfactant in the liquids. Should this be the case then the flux of surfactant in the liquids towards the interface is of order $D_1 c_1^*/R$ (where c_1^* is the characteristic volume concentration of the surfactant in the liquids) whilst the divergence of the surface flux in the interface is of order c^*U/R (where c^* is the characteristic interfacial concentration of surfactant). Thus the flux of surfactant to or from the interface from the liquids is negligible (assumption (b)) if

$$\frac{c_1^* D_1}{c^* U} \ll 1 \quad \text{or} \quad \frac{Rc_1^*}{c^*} \left(\frac{UR}{D_1}\right)^{-1} \ll 1. \quad (8.6)$$

Should transport of the surfactant in the liquids be convection dominated so that

$$\frac{UR}{D_1} \gg 1, \quad (8.7)$$

then the flux of surfactant across the boundary layer towards the interface is of order $c_1^*(D_1 U/R)^{\frac{1}{2}}$ so that the condition (8.6), for the neglect of surfactant flux to the interface, must be replaced by

$$\frac{c_1^*}{c^*} \left(\frac{D_1 R}{U}\right)^{\frac{1}{2}} \ll 1 \quad \text{or} \quad \frac{Rc_1^*}{c^*} \left(\frac{UR}{D_1}\right)^{-\frac{1}{2}} \ll 1. \quad (8.8)$$

If (8.6) or (8.8) is satisfied then the surfactant flux to the interface is negligible not only in the outer region but also in the intermediate and inner regions.

If D is the diffusion constant for the surfactant within the liquid-liquid interface, then diffusion along the interface is negligible compared with convection (assumption (d)) in all three expansion regions if

$$\frac{D}{Us} \ll 1, \quad (8.9)$$

which may be expressed alternatively as

$$Ca \gg \frac{\mu D}{\sigma s}. \quad (8.10)$$

For a typical situation with $\mu D \approx 10^{-8} \text{ g cm s}^{-2}$, $\sigma = 10 \text{ dynes/cm}$ and $s = 10^{-5} \text{ cm}$, (8.10) gives $Ca \gg 10^{-4}$ which is usually well satisfied in cases of interest for which viscous effects play any significant role.

For any given value of σ_m and $Ca \ln(\epsilon^{-1})$, the minimum value of σ predicted by the present theory (which as we have seen may occur at the wall or at the outer region) must be greater than the minimum value of σ which can be obtained by the surfactant-covered interface (assumption (e)). Thus for example for $\lambda = 0$, $\sigma_0 \cos \theta_0 = +1$ with $\sigma_m = 2$ (figure 6b, case D), if the minimum possible σ is 1.4, the theory would be valid only for $Ca \ln(\epsilon^{-1}) < 0.37$, with surfactant accumulating at the wall for $Ca \ln(\epsilon^{-1}) > 0.37$. Similarly the maximum value of σ predicted by the theory (which may occur at the wall, at the outer region or in the interior of the intermediate region) must be less than the maximum value of σ attainable (which would normally occur for zero surfactant concentration). Thus for $\lambda = 1$,

$\sigma_0 \cos \theta_0 = +1$ with $\sigma_m = 2$ (figure 6a, case B), if the maximum possible σ is 2.05, the theory would be valid only for $Ca \ln(\epsilon^{-1}) < 0.41$, with the surfactant layer breaking in the intermediate region (where $\theta = 90^\circ$) when $Ca \ln(\epsilon^{-1}) = 0.41$. For still larger values of $Ca \ln(\epsilon^{-1})$ part of the interface in the intermediate region will have no surfactant present.

The condition (3.28) for the neglect of time-dependent effects means that the theory cannot be applied at or immediately after a situation in which θ_w takes a sudden jump in value as would occur if the contact line were to meet a sudden change in the nature of the solid surface.

While in the theory described here, it was assumed that the Bond number B was small (see §2), it is readily seen that for B of order unity (see Cox 1986), the results (7.12) and (7.13) are still valid since the effect of gravity is negligible in the intermediate and inner regions. However, for this situation, the effect of gravity would have to be included in calculating the outer region expansion.

In a manner similar to the surfactant-free situation considered by Cox (1986), there is also the possibility that at distances of about 10^{-6} to 10^{-8} cm from the contact line, very high negative pressures can occur which can result in cavitation taking place. Should this occur then the theory described above would no longer be valid.

This work was supported by the Natural Sciences and Engineering Research Council of Canada under grant A7007 and was undertaken in part at the Department of Mathematics, University College London, England and at the Department of Chemical Engineering, MIT, Cambridge, Mass., USA.

REFERENCES

- BLAKE, T. D. & HAYNES, J. M. 1969 *J. Colloid Interface Sci.* **30**, 421.
 CHERRY, B. W. & HOLMES, C. M. 1969 *J. Colloid Interface Sci.* **29**, 174.
 COX, R. G. 1986 *J. Fluid Mech.* **168**, 169.
 DUSSAN, V., E. B. 1979 *Ann. Rev. Fluid Mech.* **11**, 371.
 HOCKING, L. M. 1977 *J. Fluid Mech.* **79**, 209.
 HOCKING, L. M. & RIVERS, A. D. 1982 *J. Fluid Mech.* **121**, 425.
 HUH, C. & MASON, S. G. 1977 *J. Colloid Interface Sci.* **81**, 401.
 LOWNDES, J. 1980 *J. Fluid Mech.* **101**, 631.
 NGAN, C. G. & DUSSAN, V., E. B. 1982 *J. Fluid Mech.* **118**, 27.